

W. GONG¹
J. SHI¹
G. LI¹
D. LIU^{1,✉}
J.W. KATZ²
E.S. FRY²

Calibration of edge technique considering variation of Brillouin line width at different temperatures of water

¹ Applied Optics Beijing Area Major Laboratory, Department of Physics, Beijing Normal University, Beijing 100875, P.R. China

² Department of Physics, Texas A&M University, College Station, TX 77843-4242, USA

Received: 2 December 2005/

Revised version: 22 February 2006

Published online: 29 March 2006 • © Springer-Verlag 2006

ABSTRACT Edge technique is a sensitive and accurate technique for measuring Brillouin shift in water. Calibration is necessary in its applications in remote sensing of the ocean. In previous works, the normalized signal was calibrated without considering the change of Brillouin line width under different temperatures of the water. In this work, the normalized signal of edge technique was re-calibrated basing on temperature dependence of the line width of Brillouin scattering in water. A more accurate relationship between Brillouin shift and the normalized signal was obtained.

PACS 42.68.Wt; 42.79.Qx; 78.35.+c

1 Introduction

The Lidar remote sensing technique with a frequency shift of less than one GHz was widely used in atmospheric and oceanic applications. An atomic resonance filter (ARF) is needed for measuring such small frequency shifts [1, 2]. The most commonly used atomic resonance filter is an iodine absorption cell [3, 4], and it had been successfully employed in the so-called edge technique for remote sensing of the atmosphere by Korb et al. [5–7].

Brillouin scattering [8, 9] can be used to measure sound speed and temperature of seawater [10–15]. It has the advantage over Raman scattering that the narrow Brillouin line width minimizes the effect of daylight and fluorescence [11], so it shows significant potential of being used in lidar remote sensing of the ocean. However, high resolution spectroscopy is needed for Brillouin scattering. Hirschberg used a dual Fabry–Perot etalon [11] for solving this problem. It is, in fact, analogous to the edge technique discussed in recent years. Fry et al. [14] and Liu et al. [15] did the measurements by using a high resolution scanning Fabry–Perot. However, a Fabry–Perot has a very limited solid angle for acceptance of the lidar return signal, which severely limits the capabilities of such an approach.

Under the advice of Fry [14], Liu et al. [16–18] developed an edge technique using iodine and bromine cells for measuring Brillouin shift in water. Also, Walther et al. suggested a new system with edge technique using only one cell [19]. In edge technique, the Brillouin shift is determined by normalized intensity, which depends on the transmitted intensity passing through the iodine cell [16]. The principles of edge technique is shown in Fig. 1 (for all details please refer to [16]), in which the Brillouin line width was chosen as a constant value of 500 MHz. If the Brillouin line width is changed with the change of temperature or salinity of the water, it will influence the overlap area. In this case, the transmitted intensity passing through the edge filter will be different even though the Brillouin shift remains unchanged. Therefore, the effect of the Brillouin line width on the normalized intensity of the edge technique should be considered in practical applications.

However, in previous reports about edge technique, Brillouin line width was considered as a constant though the width is actually changed with variations of temperature or salinity of the water [20, 21]. Therefore, in order to obtain more accu-

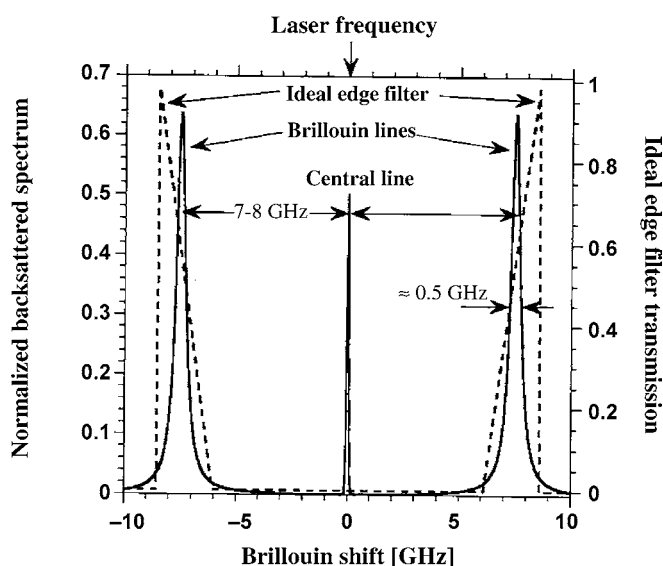


FIGURE 1 Principles of the edge technique

✉ Fax: 8610-58800141, E-mail: dhliu@bnu.edu.cn

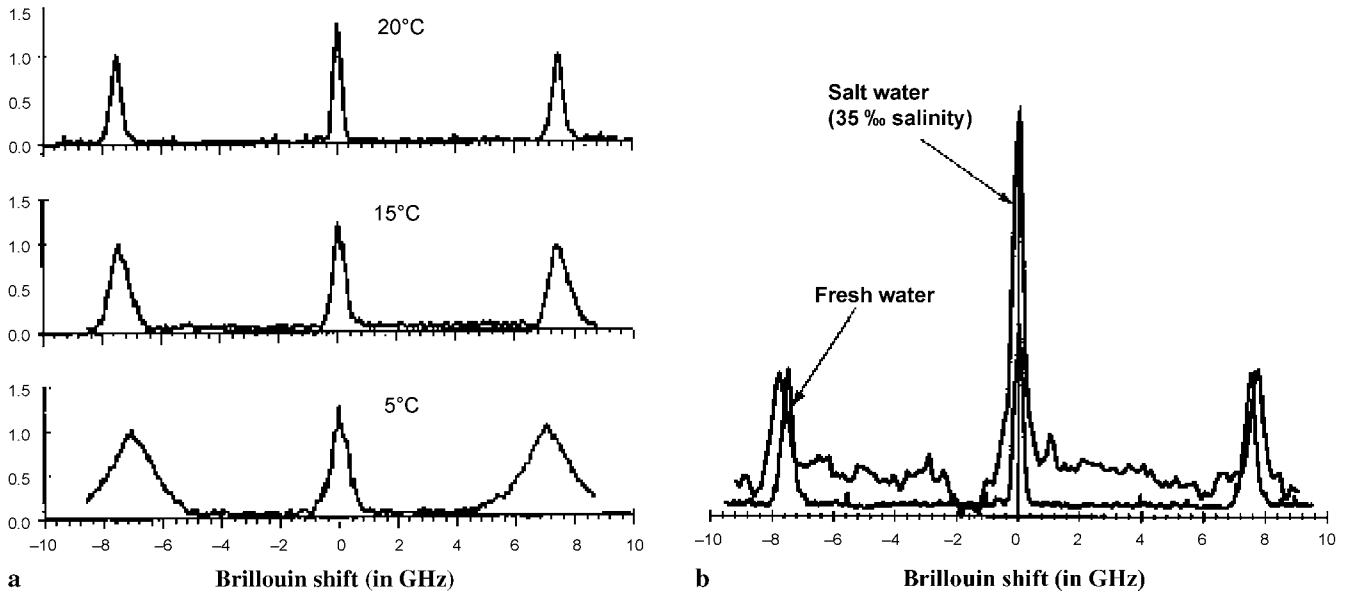


FIGURE 2 (a) The Brillouin line width and shift vs. temperature. The spectra were measured in fresh water. (b) Brillouin line width and shift vs. salinity of water. The water temperature was 20 °C

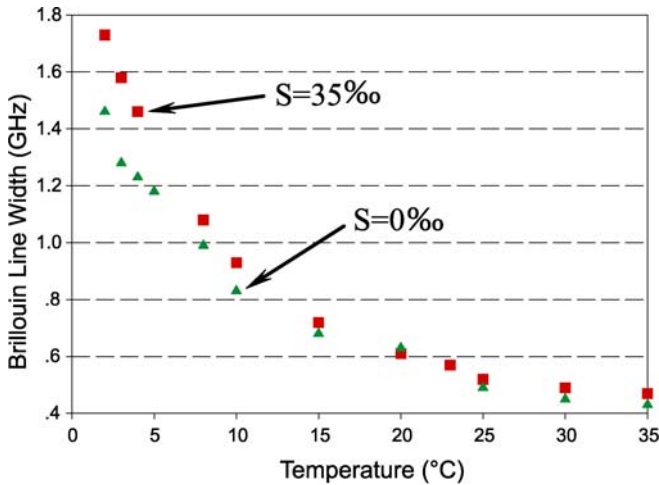


FIGURE 3 Temperature dependence of the Brillouin line width for water with different salinities

rate results, the lidar system with the edge technique should be re-calibrated with special considering of Brillouin line width. The purpose of this work is to describe the calibration of the lidar system using iodine and bromine cells by considering the temperature and salinity dependence of the Brillouin line width.

2 Temperature dependence of Brillouin line width

Temperature dependence of Brillouin line width at different salinities of the water were observed. Figure 2 gives the relationship between the Brillouin line width and the temperature and salinity of the water [20, 21]. It can be seen clearly that not only the Brillouin shift, but also the Brillouin line width is changed with the change of temperature or salinity of the water. Considering the actual case of the open ocean, the Brillouin line width in the temperature range of

2 °C through 35 °C were measured and the results are shown in Fig. 3.

The variation of Brillouin line width with temperature and salinity of the water will influence the overlap area between absorption peak of the edge filter used and the Brillouin peak in the the scattering spectrum, it is the reason why the lidar system with edge technique should be re-calibrated.

3 Calibration considering the variation of Brillouin line width

In our suggested lidar system [14, 16], the absorption spectra of iodine and bromine cells used are shown in Fig. 4. The profiles of the absorption spectra of the two cells $g_{Br}(\nu)$ and $g_I(\nu)$ were fitted form the data in the two figures. Also, the Brillouin line is a Lorentzian which is expressed as

$$f(\nu, \nu_B) = \frac{1}{\pi \Gamma_B} \left\{ \frac{1}{1 + [2(\nu - \nu_B)/\Gamma_B]^2} + \frac{1}{1 + [2(\nu + \nu_B)/\Gamma_B]^2} \right\}, \quad (1)$$

where, Γ_B is the width (FWHM) of the Brillouin line, which is supposed to have a typical value of $\Gamma_B = 0.5$ GHz. Assuming that the signal intensity transmitted through the Br₂ cell (blocker) is unity, then according to the alignment of the lidar shown in Fig. 5, the fractions of the lidar return received by the first and second detectors can be given by

$$Q_1(\nu_B) = \frac{1}{2} \int_{-\infty}^{\infty} f(\nu, \nu_B) g_{Br}(\nu) d\nu, \quad (2)$$

$$Q_2(\nu_B) = \frac{1}{2} \int_{-\infty}^{\infty} f(\nu, \nu_B) g_{Br}(\nu) g_I(\nu) d\nu. \quad (3)$$

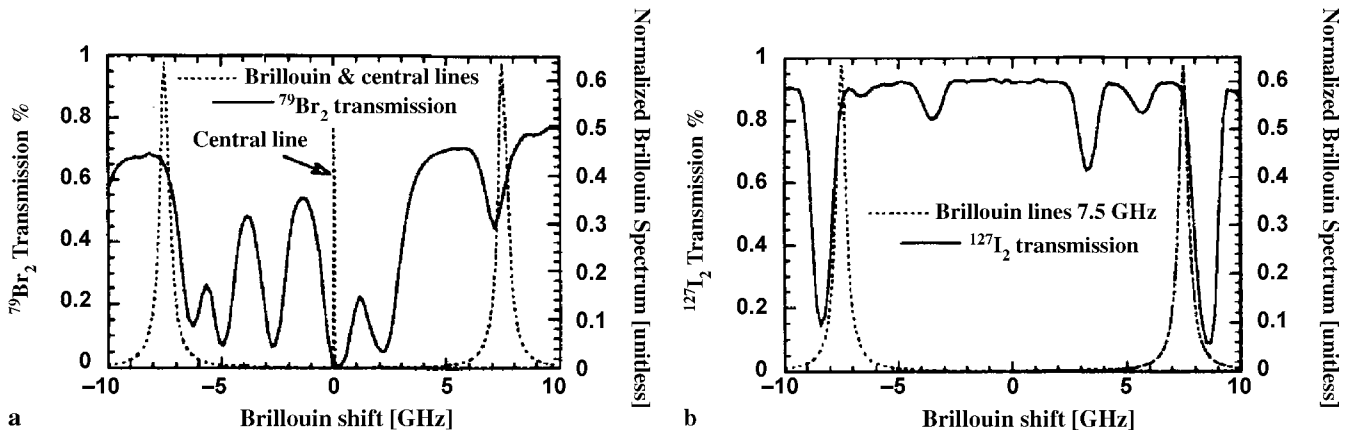


FIGURE 4 (a) Absorption spectrum of a bromine ($^{79}\text{Br}_2$) cell. (b) Absorption spectrum of an iodine ($^{127}\text{I}_2$) cell

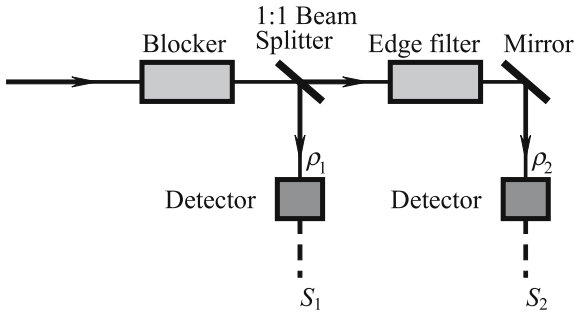


FIGURE 5 Schematic for an example system

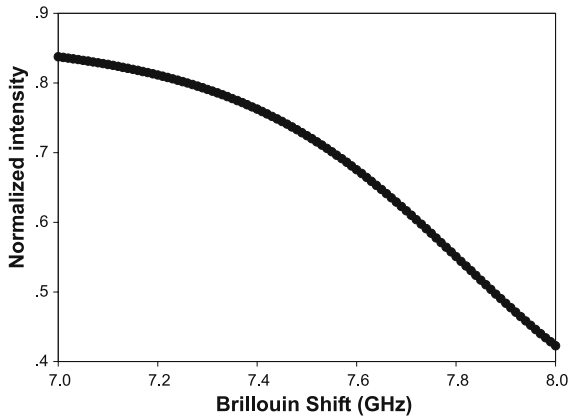


FIGURE 6 Brillouin shift dependence of normalized intensity

The observed signals are

$$S_1 = \varrho_1 N_{pe}, \quad S_2 = \varrho_2 N_{pe}, \quad (4)$$

where N_{pe} is the number of output Brillouin photo-electrons produced per pulse by an optical receiver in a pulsed laser backscattering system. A normalized signal intensity $S(\nu_B)$ is defined as

$$S(\nu_B) = \frac{S_2}{S_1} = \frac{\varrho_2}{\varrho_1}. \quad (5)$$

The Brillouin shift can be determined by the theoretical normalized intensity. Figure 6 gives the Brillouin shift dependence of the value of the normalized signal. It can be seen

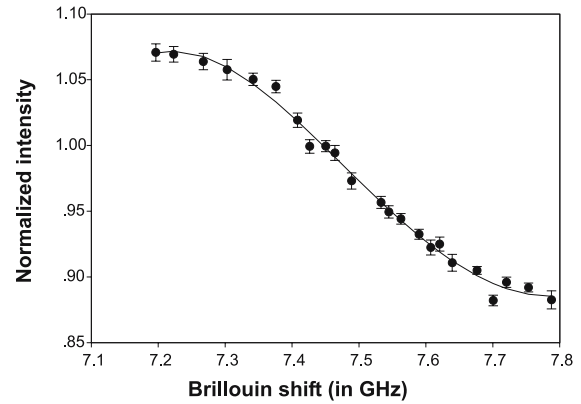


FIGURE 7 Measured data in experiments by edge technique using iodine and bromine cells

clearly that there is one-to-one correspondence between the normalized intensity and the Brillouin shift.

However, the measured data shown in Fig. 7 is obviously different from that in Fig. 6 [16]. The reason causing this difference is that the calibrated curve was derived theoretically by considering the Brillouin line width as a constant $\Gamma_B = 0.5$ GHz rather than considering the variation of the Brillouin line width with the change of water temperature and salinity. Therefore, re-calibration considering the variation of the Brillouin line width with the change of water temperature and salinity should be made so that accurate determination of the Brillouin shift can be obtained by the lidar system using iodine and bromine cells [16].

The profile of $g_1(\nu)$ was refitted basing on the concerned parts of the absorption spectrum of the iodine cell, and considering the variation of Brillouin line width at different temperatures, (see Fig. 8a), normalized intensity was recalibrated considering the influence of Brillouin line width (see Fig. 8b). The final calibrated curve is shown in Fig. 9. Moreover, according to the Fig. 4a, the bromine cell used as a blocker absorbs certain Brillouin signals. Also, compensation can be made by fitting the curve of $g_{Br}(\nu)$.

It should be noted that in actual applications, the blocker (bromine cell) and the edge filter (iodine cell) are working at certain temperatures, and the molecular concentration in the cells are controlled by temperature. The transmission of the cells are determined by the molecular concentration.

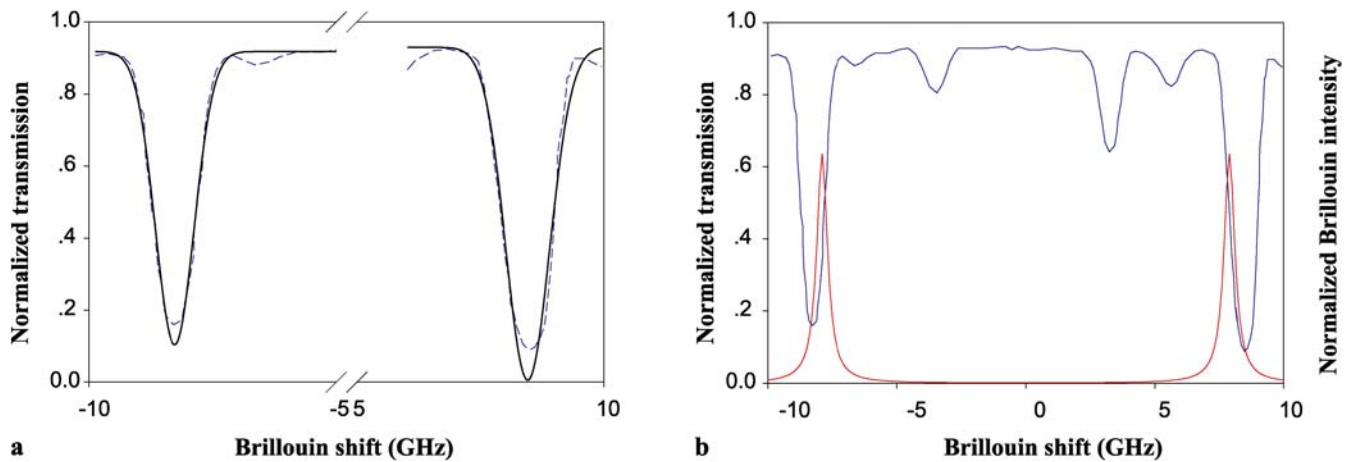


FIGURE 8 Fitting results of the edge filter using iodine cell. (a) Two concerned parts of the absorption spectrum of the iodine cell. (b) Relationship between absorption spectrum of iodine cell and the Brillouin peak of the scattered signal

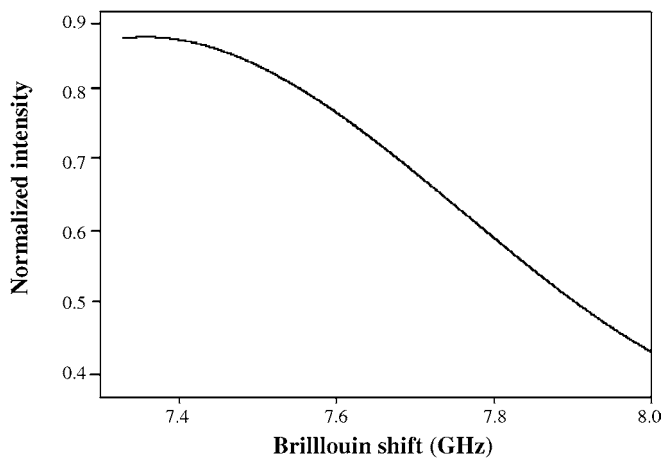


FIGURE 9 Relationship between absorption spectrum of iodine cell and the Brillouin peak of the scattered signal

The calibrated curve shown in Fig. 9 is calculated at the temperatures of the two cells used in our lidar system. Different calibrated curves may be obtained for different lidar systems.

It can be seen clearly that the calibrated curve shown in Fig. 9 is in much better agreement with the measured results shown in Fig. 7 than that shown in Fig. 6 which was calculated without consideration of the variation of the Brillouin line width at different temperatures and salinities of the water.

Here, it should be pointed out that for the measured results shown in Fig. 7, some values of the data are larger than unit. The reason is that the beam splitter used is not an accurate 1 : 1

splitter, the absorptions of the glass consisting of the two cells are not accurate the same.

ACKNOWLEDGEMENTS The authors thank the National Natural Science Foundation of China (Grant No. 10274006) and the National Advanced Technology Program (Grant No. 2002AA633110) for financial supports.

REFERENCES

- 1 J.A. Gelbwachs, IEEE J. Quantum Electron. **QE-24**, 1266 (1988)
- 2 G. Yang, R.I. Billmer, P.R. Herczfeld, V.M. Contarino, Opt. Lett. **22**, 414 (1997)
- 3 P. Piironen, E.W. Eloranta, Opt. Lett. **19**, 234 (1994)
- 4 J.N. Forkey, W.R. Lempert, R.B. Miles, Appl. Opt. **36**, 6729 (1997)
- 5 C.L. Korb, B.M. Gentry, C.Y. Weng, Appl. Opt. **31**, 4202 (1992)
- 6 C.L. Korb, B.M. Gentry, X. Li, Proc. SPIE **2310**, 206 (1994)
- 7 J.S. Friedman, C.A. Tepley, P.A. Castleberg, H. Roe, Opt. Lett. **22**, 1648 (1997)
- 8 L. Fabelinskii, *Molecular Scattering of Light* (Plenum Press, New York, 1968)
- 9 I.L. Fabelinskii, Prog. Opt. **XXVII**, 95 (1997)
- 10 J.G. Hirschberg, J.D. Byrne, A.W. Wouters, G.C. Boyton, Appl. Opt. **23**, 2624 (1984)
- 11 J.G. Hirschberg, J.D. Byrne, Proc. SPIE **489**, 270 (1984)
- 12 D.J. Collins, J.A. Bell, R. Zanoni, I.S. McDermid, J.B. Brecknidge, C.A. Sepulveda, Proc. SPIE **489**, 247 (1984)
- 13 G.D. Hickman, J.M. Harding, M.C. Garnes, A. Pressman, G.W. Kattwar, E.S. Fry, Remote Sens. Environ. **36**, 165 (1991)
- 14 Y. Emery, E.S. Fry, Proc. SPIE **2963**, 210 (1997)
- 15 D. Liu, J. Xu, R. Li, R. Dai, W. Gong, Opt. Commun. **203**, 335 (2002)
- 16 R. Dai, W. Gong, J. Xu, X. Ren, D. Liu, Appl. Phys. B **79**, 245 (2004)
- 17 J. Xu, R. Dai, W. Gong, X. Ren, D. Liu, Appl. Phys. B **79**, 131 (2004)
- 18 W. Gong, R. Dai, Z. Sun, X. Ren, J. Shi, G. Lin, D. Liu, Appl. Phys. B **79**, 635 (2004)
- 19 A. Popescu, K. Schorstein, T. Walther, Appl. Phys. B **79**, 955 (2004)
- 20 J. Xu, X. Ren, W. Gong, R. Dai, D. Liu, Appl. Opt. **42**, 6704 (2003)
- 21 E.S. Fry, J. Katz, D. Liu, T. Walther, J. Mod. Opt. **49**, 411 (2002)